Journal of Rehabilitation in Civil Engineering 7-1 (2019) 70-82

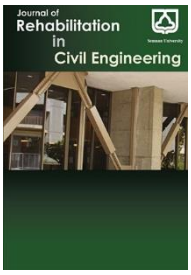

journal homepage: http://civiljournal.semnan.ac.ir/

Experimental Assessment of Partially Encased Composite Columns Behavior under Compressive and Bending Moment Loading

M. Ebadi Jamkhaneh[1] and M. A. Kafi[2*]
1. Assistant Professor, School of Engineering, Damghan University, Damghan, Iran.
2. Associate Professor, Faculty of Civil Engineering, Semnan University, Semnan, Iran.

Corresponding author: *mkafi@semnan.ac.ir*

ARTICLE INFO

Article history:
Received: 19 September 2017
Accepted: 31 October 2017

Keywords:
Partially Encased Composite Column,
Failure Mode,
Experimental Model,
Load Bearing Capacity,
Concrete Reinforcement.

ABSTRACT

In recent years, Partially Encased Composite columns are evaluated as new achievements in the field This paper presents a combined experimental and theoretical study on the mechanical performances of six octagonal PEC columns subjected to axial compressive and bending moment loading. The main difference between them was the details of concrete strengthening. In the experimental study, the parameters investigated were the sort of detail of strengthening and the mode of failure. The results were represented as load-deformation and moment-rotation curves. The test results were compared with the measurements of relations captures from CSA S16-14 and EN 1994-1-1 codes. The comparison of the code equations given in CSA S16-14 and EN 1994-1-1 revealed that the equation in CSA S16-14 underestimates the capacity. Also, the failure mode was similar for all three concentrated tests: concrete cracking coupled with the steel flange buckling.

1. Introduction

One of the new achievements of the construction of composite column is partially encased composite (PEC). These are made of thin-walled plates which is infilled with concrete. The plates are welded thoroughly along the column axis. The links between the flanges are spaced at regular intervals to enhance the resistance of the flanges to local buckling. The new system also differs from PEC column currently applied in European practice as the latter is made with hot-rolled standard W-shapes not prone to local buckling . The Canam Group has recently created a new form of PEC column, primarily to withstand compressive axial loading in mid- and high-rise structures. Design rules have been created for PEC columns and integrated into the Canadian steel design standard, S16-01 [1]. Few

DOI: 10.22075/JRCE.2017.12538.1216

studies have carried out experimental and numerical PEC models in latest years.

A series of PEC columns under bending moment and reversed cyclic loads were examined[2-5]. The joint performance of PEC beams to the PEC column was explored [6,7]. The PEC column with thinner thickness of steel walls rather than that of PEC column which is fabricated in Europe, with greater link intervals manifests a quicker strength degradation after peak load than columns with closer link spacing [8]. Chicoine et al. [9] designed a mathematical model to seek the influence of flange imperfections and residual stresses on the column behavior. In addition, Chicoine et al. [10] inspected the PEC column behavior incorporating of different factors such as spacing of the links, flange stiffness, and longitudinal rebars. Some experimental studies were manifested by Prickett and Driver [11] for studying the behavior of PEC columns with considering the link intervals, load eccentricity and concrete strength. They compared the test results with modified load-moment curves which the brittle mode behavior of the columns was revealed. A parametric study on PEC columns under bending moment loading was conducted by Begum et al. [12]. A set of numerical studies and experimental tests on partially composite columns under cyclic accompanied with compressive loading performed by Chen et al. [13]. Their results revealed the existence of links interval led to avoid buckling flange. In 2012, the compressive behavior of PEC columns was examined by Zhao and Feng [14]. The results indicated that a close distance between links improves the ductility of column. Whereas, the overall fracture in the link does not occur before the peak load. Other researchers [15] applied the PEC columns as the boundary elements for steel shear wall system. In this study, enhancement of the seismic performance of the system is due to the application of PEC column. The behavior of PEC columns detailed with longitudinal bars and stirrups inspected under axial loading by Pereira et al. [16]. Their results revealed detailing reinforcement of column has no significant influence on load-carrying capacity and stiffness of the PEC column. Song et al. [17] performed parametric study on buckling behavior of PEC column which made of steel welded plates. Their study led to statements for anticipating critical strength and buckling after maximum strength.

In previous studies, most of research focused on behavior of PEC columns made of normal manufactured section and plates with an equal thickness. Despite all the mentioned research, the effect of varying thin-walled thickness, steel section shape, and welding line length is missing in rigorous research. Same stiffness in both ways, section symmetry, simple application, and possible connection in any direction, distinct thicknesses for flanges and webs are applied in this paper for cruciform type steel profile. It is noteworthy to mention that under axial and eccentrically compressive load; the suggested column is examined. The low torsional resistance of the cross-shaped steel section is one of the main drawbacks. The tips of flanges were connected with links. In order to ameliorate the torsional strength of section, concrete was used between the plates. The significant goals of the test study are to capture a better comprehending of the effect of concrete reinforcement on the behavior of the PEC column and to capture the effects of concrete on the compressive and bending moments, and to propose a new PEC column shape and to develop an efficient and economical procedure to

enhance structural speed erection. In the following parts of this study, details of the research were described.

2. Test Study

Six 1/3 scale PEC columns measuring (width × depth × height) 150 mm×150 mm × 1000 mm were built. Figure 1 depicted geometric parameters typical of the PEC column. The parameters given in the elevation view of the concrete side (Figure 1(a)) are the column height, L, and the distance between the axis of links, s. Column depth, d, overall flange width, b_f, thickness of web and flange, t_f and t_w, are parameters displayed in the plan perspective (Figure 1(b)). The steel part was manufactured from grade st37. The thickness of flange was 6 mm and this measure is 3 mm for web plate. The nominal proportion of the width to thickness of the column flange was 10. The value in CSA S16-14's [18] which has a maximum slenderness of flange of 32, is higher than that. All spacing between the links was selected as 100 mm and has a diameter of 6 mm. The transverse links are laid back from the flange tips so that, irrespective of the link diameter, there is 10 mm of clear concrete cover between the link and the concrete face. Furthermore, flange width equivalent to 60 mm. Columns were casted in the test region with ordinary concrete strength (nominally 25 MPa). Table 1 presents a summary of the PEC columns characteristics. Stiffeners have reinforced the end areas of the columns (50 mm of column length at each end) to avoid possible failure owing to irregular loading at these places.

2.1. Concrete Property

During the mix design, the workability and were the primary characteristics of concern. Table 2 reveals the portions of materials in concrete mixture design. The concrete was produced of 12.5 mm crush coarse aggregate materials accessible locally. The fine sand module is 2.4.

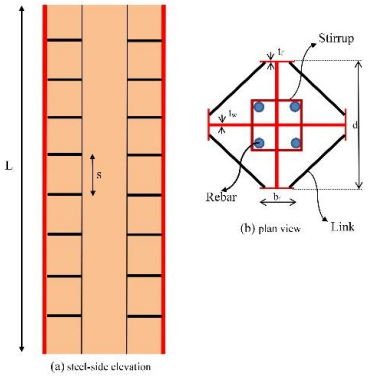

Fig. 1. (a) elevation scheme, and (b) plan view of PEC column

Considering that the typical concrete density of the mixes was 2300 kg/m^3, the elastic concrete module (23715 GPa) is in the span of the Concrete Practice Report ACI-318-08 of the American Concrete Institute (ACI) [19]. The ordinary strength concrete's average strain at peak stress is 2225 micron, which is a typical value. In consonance to the ACI report 363R-92, the Poisson normal-strength concrete proportion (0.13) is typical of accepted values (0.11 to 0.21) for normal-strength concrete [20].

Table 1. Features of experimental samples.

Column		PEC-1	PEC-2	PEC-3
Longitudinal bar	Number	0	4	4
	Diameter (mm)	0	14	14
Stirrup	Spacing (mm)	0	0	100
	Diameter (mm)	0	0	6

Table 2. Concrete mix design.

Material	Water	Cement	Gravel	Sand	W/C ratio
Mass (kg)	215	430	1053	617	0.5

2.2. Steel Properties

All coupon experiments were carried out at the Semnan University Structural Engineering Laboratory. Typical of hot-rolled structural grade steels are the stress -strain curves produced. From the steel bars, four tension coupons were examined. The other two were trimmed as longitudinal rebar from the 14 mm steel rod. The coupons were evaluated as presented in Table 3 in accordance with ASTM Standard A370 [21]. In addition, welding was carried out applying electrodes with final strain and tension of welds as 0.6% and 420 MPa, respectively.

Table 3. Tensile coupon test for steel rod and plate.

	Yield Stress (MPa)	Ultimate Stress (MPa)	E (MPa)	Failure Strain (με)	Rupture Strain (με)
Plate	257	389	202100	1951	320000
Bar	297	412	195600	1568	451000

3. Loading and Test Setup

Three columns (PEC-1 through PEC-3) were examined on one hand with a fixed-end condition and on the other side with a vertical slide. Eccentric loading (pure bending moment and compressive-bending loading) evaluated the remaining six PEC columns. The two test setups required a fundamentally various arrangements. A test system machine with a loading capacity of 2 MN was applied to test the three columns under concentrated compressive loading. The hydraulic jack with maximum stroke of 400 mm utilized for applying the axial compressive loading.

For each of the three tests, the loading method was similar. The UTS was controlled by primary force level (5 kN/min). The test started at a load level of 50 kN/min until the deformation attained about 0.05 mm. Subsequently, the load rate grew up to 75 kN/min until the column behavior's plots indicated a decrease in column stiffness (normally about 80 percent of the peak load). The load rate was reduced to the start load rate until column failure happened to minimize dynamic effects. The UTS load remained constant until the displacement of the measured UTS had stabilized and photographs taken. At a stroke speed of 0.06 mm/min, loading was then alternated to displacement command. If the failure resulted in a slow decrease in ability, the stroke speed was maintained at 0.06 mm/min until the column strength was lowered to below 85% of the maximum load. The speed then rose to 0.08 mm/min. Irrespective of the sort of failure, the stroke speed was amended to 0.1 mm/min once the degradation of the post-peak force started to decrease considerably. Then the load was reversed. Figure 2 demonstrates the sample configuration for concentrated load. For each of the three bending moment tests, the loading procedure was similar. Throughout the experiment, the loading method was comparable to the concentration load procedure. The vertical loading was exerted to the column on a stiff beam (Figure 3).

(a) Position of hydraulic jack (b) Specimen layout

Fig. 2. Setup for concentric compression loading.

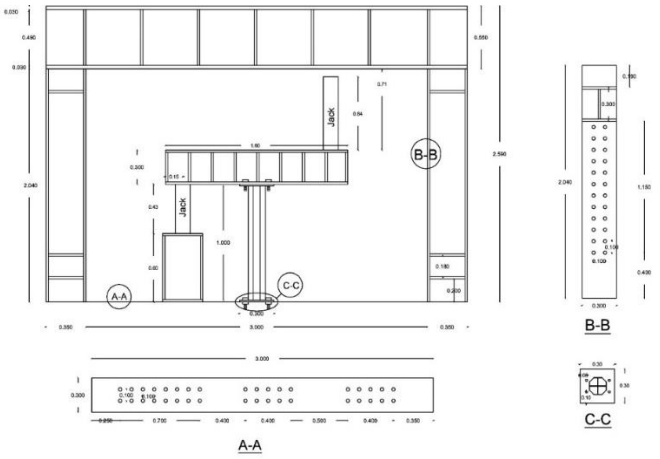

Fig. 3. Setup for pure moment loading (Units: mm).

4. Experimental Results and Discussion

4.1. Results of Concentric Loading

4.1.1. Comparison Between Relations and Test Results

The overview of the maximum specimen loads and anticipated loads for the three concentrated PEC columns (CSA S16-14 [18] and EN 1994-1-1 [22]) is provided in Table 4. Applying Eqs., the expected force was computed (1) and (2) respectively.

$$C_{rc} = \left(\phi A_{se} F_y + 0.95\alpha_1 \phi_c A_c f_c' + \phi_r A_r F_{yr}\right)\left(1+\lambda^{2n}\right)^{1/n}$$

CSA S16-14 (1)

$$N_{pl,Rd} = A_a f_{yd} + A_s f_{sd} + 0.85 A_c f_{cd}$$ EN1994 (2)

$N_{pl,Rd}=C_{rc}$=the factored compressive strength, ϕ=0.90, ϕ_c=0.65, ϕ_r=0.85, A_r=longitudinal bar area, A_{se}=influential region of the steel section, A_c=concrete area, f_{sd} and F_y are the yield strength of plate, $f_{yd}=F_{yr}$=failure stress of steel rebar, $f_{cd}=f'_c$=compressive strength of concrete, λ=slenderness parameter, α=0.85 -0.0015f'_c, and n=1.34.

$$\lambda = \sqrt{C_p / C_{ec}} \quad (3)$$

$$C_{ec} = \left(\pi^2 EI_e\right) / \left(KL\right)^2 \quad (4)$$

$$EI_e = \left(0.6 E_c I_c\right) / \left(1 + \left(C_{fs} / C_f\right)\right) + EI_s \quad (5)$$

C_{fs} is axial exerted load, C_f is total load, I_s is the moment of inertia of steel and I_c is the inertial moment of the concrete. Parameters of C_p and C_{rc} computed with ϕ_c, ϕ, and ϕ_r= 1.0 and λ=0. C_{ec} is critical loading and E_c and E are modulus of elasticity of concrete and steel.

Slenderness parameter for calculating the column capacity has been set to zero. The experimental load passed from the expected capacity of the CSA S16-14 relation for all three sample samples. The steel rebar columns, PEC-2 and PEC-3, have the largest experimental to anticipated load in according to the equation proportions of CSA S16-14, 1.23 and 1.32, respectively. Canadian concept computations decrease the strength of flange to compensate for their predisposition to bulging of the transverse bars.

4.1.2. Load-Displacement Curves

Figure 4 reveals the three concentrated test samples' axial load-displacement reactions. For each sample, the measurements of initial stiffness, peak stress and displacement are presented in Table 5. The primary stiffness was obtained within the elastic range of the load-displacement response from a linear regression study. Specimen PEC-3 showed the highest strength, approximately 1.47 and 1.07 times that of Specimens PEC-1 and PEC-2. In the PEC-3 sample, which was 24 times greater than that of the PEC-1 sample, the greatest initial stiffness was also observed.

Table 4. Comparison of maximum load-carrying capacity between computed and test results.

Sample	$P_{(Exp)}$ (kN)	$P_{(CSA)}$ (kN)	$P_{(EN)}$ (kN)	$P_{(Exp)}/ P_{(CSA)}$	$P_{(Exp)}/ P_{(EN)}$
PEC-1	803	688	876	1.17	0.92
PEC-2	1105	896	1117	1.23	0.99
PEC-3	1180	896	1117	1.32	1.06

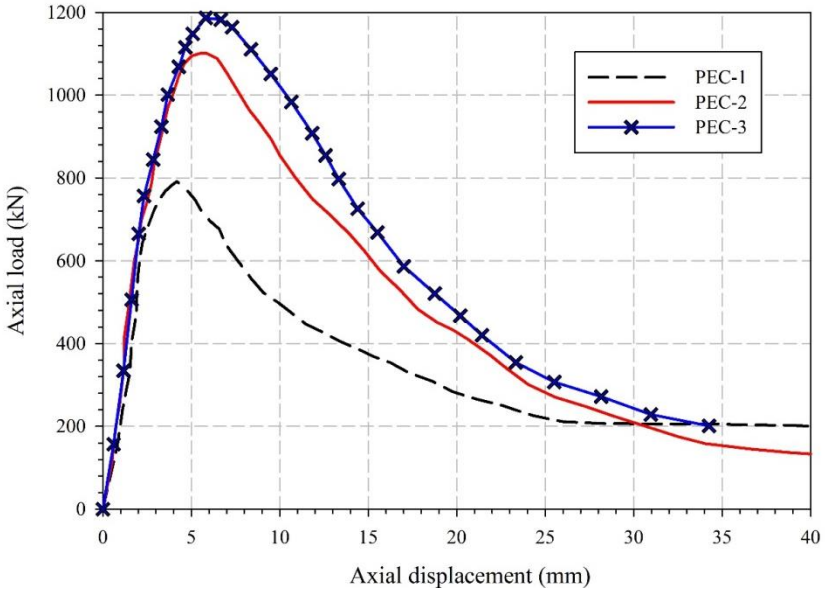

Fig. 4. Force-displacement relationships of the samples.

The higher stiffness of the PEC-3 column compared to other columns results from the application of transverse bars surrounding the bars which parallel to axis of the column, which contributes to greater confinement and thus reduces the power of the column. The existence of concrete in PEC samples has also been noted to reduce lateral deflections by 70 percent.

Table 5. Test results.

Sample	Load (kN)	Displacement (mm)	Stiffness (kN/mm)
PEC-1	803.0	4.0	216.6
PEC-2	1105.0	5.4	234.2
PEC-3	1180.0	8.7	269.5

4.1.3. Failure Modes

Similar failure mode including of concrete spalling combined with buckling of the flanges (except for column PEC-1) was seed in all specimens. No local flanges buckling was noted before the maximum force was attained for any of the columns. Although the distortion states for all columns were close, the stage at which the failure happened was distinct from the maximum capacity based on the existence or lack of steel reinforcements. Specimens at their maximum load indicated abrupt inability. The failure region was typically situated between neighboring transverse bars (Figure 5(a)). Separate shear failure surfaces were revealed by picking up the broken concrete after the experiment. The shear plane altitudes linked to the spacing of the link. The failure of shear line was only as big as the links themselves for the nearest connection spacing. This led in tiny quantities of spalling concrete off the column. Notwithstanding, the failure line expanded to a place slightly closer to the web than the concrete surface for the biggest link interval or fracturing of links. As failure occurred, big parts of concrete exploded out of the column. The relationship between the link spacing and the shear-plane depth was anticipated.

There was slight cracking at the bottom of the column before maximum loading in the PEC-1 sample. There was an abrupt decrease in capacity suddenly after the maximum load (803.0 kN) was reached. Side flanges were buckled at peak load and the concrete close to the column's left side was broken (Figure 5(a)). When the load exceeded 600 kN, two bumps were heard as the linking welds broke. Web plates were buckled at the bottom of the column at 200 mm during the post-peak loading. Immediately afterwards, the bottom flange buckled at 480 kN close the end support. The flanges were broken near the top of the test. By fracturing the welds, the unsupported length of the flange increased, resulting in the flange being ultimately buckled; the lengths of this fractured zone were about 300 mm, which gradually extended into adjacent zones. During the PEC-2 specimen failure, at first 200 mm, cracks were obvious and pulling out of the concrete occurred in this region (Figure 5(b)). The concrete close the base was cracked after a sudden fall in capacity and the top and lower flanges were buckled. A lateral crack was extended along the axis of the transverse bars during the post-peak loading. During the post-peak period, the fillet welded between the plates was broken.

Moreover, at maximum load, longitudinal rebar buckling happened, resulting in concrete cracking and spalling. In the PEC-3 sample, slight pull out of the concrete occurred at 800 kN before capacity load reached the maximum load, which began to propagate longitudinally at 950 kN. The concrete cover pulled out in the mid-height

and at the bottom part immediately after the peak load and a large segment of concrete pulled out the vicinity of the bottom of the column (Figure 5(c)). As this happened, there was flanges buckling at the support section. Simultaneously, during the test, the fillet welds failed at 140 kN between the transverse links.

Fig. 5. Buckling of flanges, crushing concrete, and fracturing in samples: (a) PEC-1, (b) PEC-2, (c) PEC-3.

4.1.4. Ductility

A ductility index (DI) suggested by Han [23] is also accepted in this document to explore the influence of steel reinforcement on the ductility of octagonal PEC columns and the associated value is described as follows:

$$DI = \frac{\varepsilon_{0.85}}{\varepsilon_u} \quad (6)$$

when the force reduces to 85 percent of the final capacity, the axial strain was shown with $\varepsilon_{0.85}$. ε_u is the strain at the final force. Figure 6 portrayed the DI calculated by Eq. (6) for all samples evaluated where a higher DI value suggests a slower load decrease technique following peak load. The DI value increases by 1.5% when the longitudinal reinforcements are attached to the concrete when comparing the PEC-2 samples with PEC-1. In addition, the DI rises by 14.6% when the PEC-3 sample compared to PEC-2. A greater steel proportion can then be discovered to lead to greater ductility.

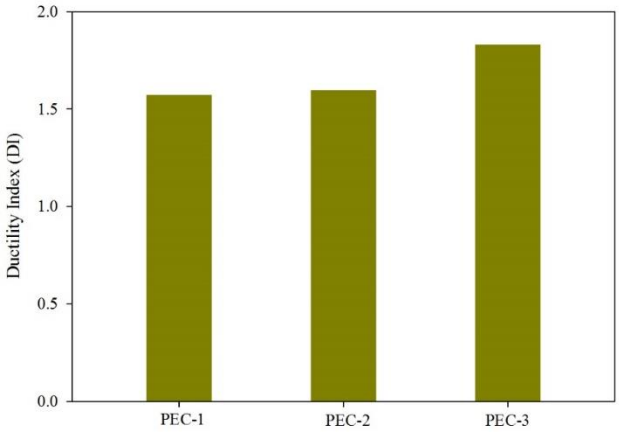

Fig. 6. Comparison of ductility index DI for all specimens.

4.1.5. Comparison of Column Behavior to Constituent Behavior

PEC column resistance is a summation of steel segment strength and concrete segment strength (see Eqs. 1 and 2). Observations generated during experiments and data from measurement evaluation indicate that there was generally no buckling before the maximum load. Relation of steel and concrete materials can be accompanied as a means of studying the general behavior of the column. Figure 7 illustrates the superimposed constituent strengths for all specimens. The concrete resistance is calculated from the median cylinder test that combined with multiplying the concrete region, A_c, by the respective measured concrete stress, f_c. Similarly, the resistance of the steel plate and rebar is computed by the steel stress, F_s and

F_r, estimated from the stress tests, multiplying A_s and A_r. At the maximum force for each column, F_s equals F_y and f_c equals f_c'. In comparison with the real column behavior, two combinations of superimposed component forces are manifested . The steel and concrete resistance plots are paired pursuant to Equation 2. The summation of the behavior of the material offers a straightforward model for comparison with the behavior of the real column.

For column PEC-1, the measured column load for the large proportion of the pre-peak behavior is lower than that anticipated by $0.8A_cf_c+A_sF_s$ and at low column loads is close to this value. The column consequently applies the entire steel section. At a higher strain, the column reaches its peak load than predicted by the summation of the component (see Figure 7(a)). The column's higher strains are as a result to the concrete confinement supplied by the link spacing. Hence, the existence of links enhanced the PEC column failure mode. Past the maximum column load, the projections of the component summation fall quickly as no confinement benefits the concrete model. A 15% rise in strain at maximum load was noted in these columns due to the application of four axial bars in column PEC-2 and the existence of transverse reinforcements in column PEC-3 (Figures 7(b) and (c)). The linear behavior of both samples was consistent with $A_rF_r+A_sF_s+0.8A_cf_c$ summation equation. It is nearly impossible to compare post-peak behavior because the predictions of the component summation did not achieve the strain at maximum load.

4.2. Results of Samples under Bending Moment Loading

4.2.1. Moment- Rotation Curves

Figure 8 demonstrates the graphs of bending moment capacity for the three columns studied between the base moment of the column and the head rotation. Bending moment is established by placing two loads one meter apart from each other on either side of the column. The figure indicates that, following a nonlinear trend, the presence of the concrete part increases the moment capacity. Also observed in the PEC-2 sample was the largest initial bending stiffness.

By applying longitudinal bars in column PEC-2 and transverse reinforcements in column PEC-3, an improvement in peak strength of 4% and 15% was noted compared to column PEC-1 respectively. Despite that, in strengthened samples, the improvement of deformability and rotational capability is much more obvious ; the existence of bars parallel with the column axis and stirrups improves the specimens' compressive stress and rotational capacity much more than it meliorates their moment capacity.

The measured stiffness (curve slope) should be close to the initial theoretical stiffness. By adding the steel portion stiffness to the concrete stiffness as follows, the theoretical initial stiffness can be calculated as follow:

$$(EI)_{PEC} = E_C I_C + E_r I_r + EI_S \quad (7)$$

In Eq. (7), $(EI)_{PEC}$ is the theoretical initial stiffness of the column, I_s, I_c, and I_r are the moment of inertia of the steel, concrete, and rebar. E, E_c, and E_r are the elastic module of the steel plate, concrete, and rebar. To compute I_c, the tensioning stiffness of the concrete is overlooked as stress formation occurs at small stresses. For columns PEC-1

through PEC-3, the initial theoretical stiffness is 1450 kN-m^2 and 1452 kN-m^2, respectively.

For all columns, the primary expected stiffness of the column is 1088 kN-m^2 in CSA S16-14. The numbers are also 1018 kN-m^2 for PEC-1 and 1163 kN-m^2 for PEC-2 and PEC-3 pursuant to the EN 1994-1-1 code. The initial stiffness of the measured columns is 1108, 1127, and 1134 kN-m^2 respectively for PEC-1 through PEC-3. The measurements of EC relations are lower than the stiffness computed as theoretical by 23%, 22%, and 22%, respectively for columns PEC-1, PEC-2, and PEC-3, as the theoretical values do not contemplate the geometric defects and material discrepancy present in the real columns.

4.2.2. Longitudinal Strain Profiles

Concrete cracks influenced the surface stress test measurements in the PEC-1 sample, as also appeared in the PEC-2 and PEC-3 samples as a result to horizontal cracks in the concrete. At peak load, all forms of PEC columns had similar stresses. The column failure mode was enhanced by adding steel reinforcement to the normal strength concrete. It was also mentioned that in any of the specimens, the web strain of the cross-shaped steel section did not achieve yielding strain.

4.2.3. Failure Mode

At a force level of 45 kN in the PEC-1 column, a deep crack was observed; subsequently the cover spalled in the top part of the column near the connection of column to beam. As presented in Figure 9(a), concrete distortion is noted to be more apparent in the bottom areas of the columns and at the end of the loading there is an increase in paint removal.

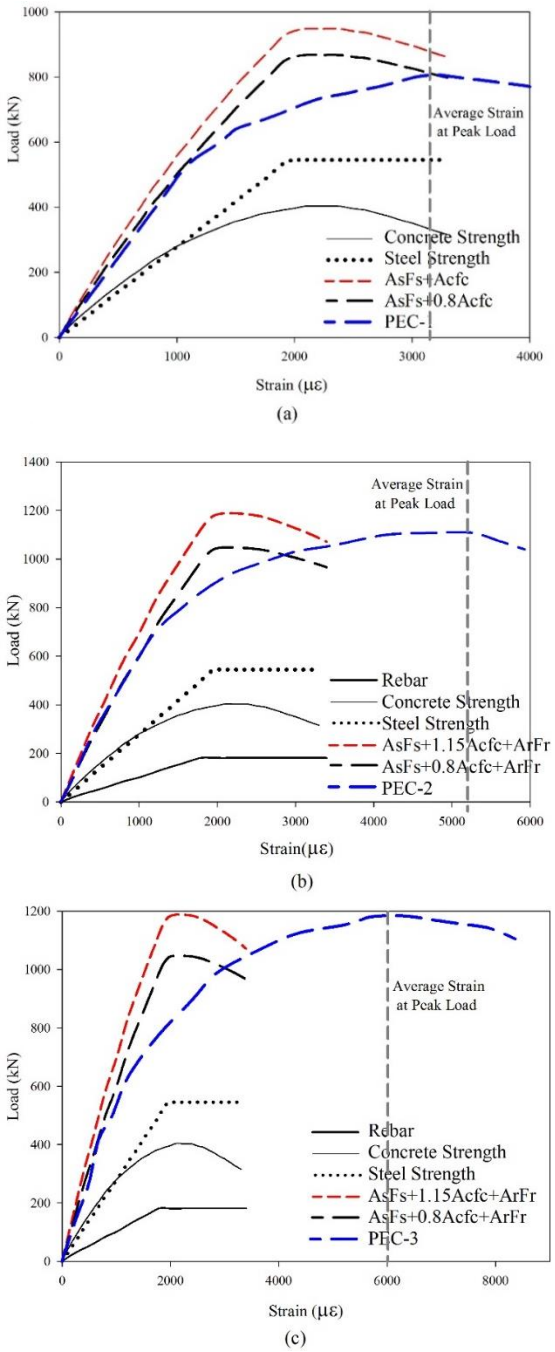

Fig. 7. Analytical resistance of PEC samples: (a) PEC-1, (b) PEC-2, and (c) PEC-3.

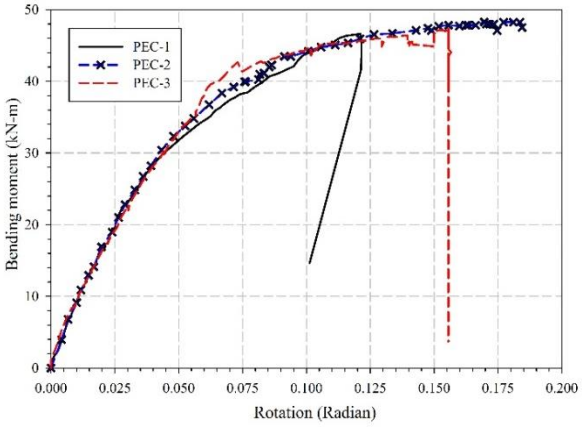

Fig. 8. Moment-rotation curves.

Nothing occurred in the PEC-2 column before the load of 37 kN; but soon thereafter color removal occurred at both sides of sections of the middle and top parts. Buckling occurred at a force level of 42 kN in the close of the beam to column zone corresponding to 64 mm deformation. After some loading, it was observed that the welding of transverse link fractures in the buckled spot and spalled of the concrete (Figure 9(b)). Deep cracks were produced by two sides of concrete spalled in compression and two other surfaces. This observation results from bigger concrete bracing spans (200 mm). In the PEC-3 column at a load level of 42 kN, cracking of the covering surface in the bottom parts of the column was noted, (Figure 9(c)). Afterwards, partial buckling and load decrease took place at a peak force level of 48 kN.

(a) (b) (c)

Fig. 9. Final stage of columns under bending loading, (a)PEC-1, (b)PEC-2, (c)PEC-3.

5. Conclusion

To study the conduct of PEC cross-shaped columns produced with varying details, an experimental research project was operated . A total of six columns of PEC have been evaluated. The modes of failure, load-strain responses, strength of the column and capacity of rotation have been discussed. The following findings from this research could be taken:

The failure mode was comparable for all three concentrated tests: concrete crushing coupled with the buckling of the steel flange. After or at the same moment the maximum load happened between the links, local buckling happened.

Adding steel bars to the concrete resulted in a slightly more ductile column failure; consequently, the PEC-2 column's failure mode was affected by the concrete's failure mode within the column. The load capacity and corresponding displacement of all samples achieve the highest value in column PEC-3.

The PEC columns were produced with normal type of concrete (without strengthening) were predicted to have an average capacity percentage of 1.14. The average proportion for rebar concrete reinforcement was 1.02. This equation is adaptable for applying with PEC columns by comparing the sample results of this research with CSA S16-14 relation. These layout calculations decrease the steel flanges' capacity to account for their susceptible links to local buckling. Nonetheless, before the peak load, flange buckling was not indicated

REFERENCES

[1] CSA. (2001). CSA S16-01, Limit states design of steel structures. Canadian Standards Association, Rexdale, ON.

[2] Hunaiti, Y.M., Fattah, B.A., (1994). “Design considerations of partially encased composite columns.” Proc., Institute of Civil Engineers, Structures and Buildings, Vol. 106, Issue 2, pp. 75-82.

[3] Elnashai, A.S., Broderick, B.M., (1994). “Seismic resistance of composite beam-columns in multi-story structures. Part 1: Experimental studies.” Journal of Constructional Steel Research, Vol. 30. Issue. 3, pp. 201-229.

[4] Chen, Y., Wang, T., Yang, J., Zhao, X., (2010). “Test and numerical simulation of partially encased composite columns subject to axial and cyclic horizontal loads.” International Journal of Steel Structures, Vol. 10, Issue. 3, pp. 385–393.

[5] Bouchereau, R., Toupin J.D., (2003). “Étude du comportement en compressionflexion des poteaux mixtes partiellement enrobés.” Report EPM/CGS-2003-03, Dept. Of Civil Engineering, École Polytechnique, Montreal (in French).

[6] Plumier, A., Abed, A., Tilioune, B., (1995). “Increase of buckling resistance and ductility of H-sections by encased concrete.” Behaviour of Steel Structures in Seismic Areas: STESSA ’94, ed. by F.M. Mazzolani and V. Gioncu, E&FN Spon, London, pp. 211-220.

[7] Muise, J., (2000). “Behaviour of simple framing connections to partially concrete encased H section columns.” Master’s Thesis, Dept of civil engineering, University of Toronto, Toronto, Canada.

[8] Tremblay, R., Massicotte, B., Filion, I., Maranda, R., (1998). “Experimental study on the behaviour of partially encased composite columns made with light welded H steel shapes under compressive axial loads.” Proc., SSRC Annual Technical Meeting, Atlanta, pp. 195-204.

[9] Chicoine, T., Tremblay, R., Massicotte, B., Ricles, J., Lu L.W., (2002). “Behaviour and strength of partially encased composite columns with built up shapes.” Journal of Structural Engineering, Vol. 128, Issue. 3, pp. 279-288.

[10] Chicoine, T., Massicotte, B., Tremblay, R., (2002). “Finite element modelling and design of partially encased composite columns.” Steel and Composite Structures, Vol. 2, Issue. 3, pp. 171-194.

[11] Prickett, B.S., Driver, R.G., (2006). “Behaviour of partially encased composite columns made with high performance concrete.” Structural engineering report No 262. Dept of civil and environmental engineering, University of Alberta, AB, Canada.

[12] Begum, M., Driver, R., and Elwi, A.E. (2015). "Parametric study on eccentrically-loaded partially encased composite columns under major axis bending", Steel and Composite Structures, An International Journal , Vol. 19, Issue, 5, pp. 1299-1319.

[13] Chen, Y., Wang, T., Yang, J. and Zhao, X., (2010). "Test and numerical simulation of partially encased composite columns subject to axial and cyclic horizontal loads", International Journal of Steel Structures, Vol. 10, Issue, 4, pp. 385-393.

[14] Zhao, G.T., Feng, C., (2012). "Axial ultimate capacity of partially encased composite columns," Applied Mechanics and Materials, Vol. 166-169, pp. 292-295.

[15] Dastfan, M., Driver, R., (2016). "Large-scale test of a modular steel plate shear wall with partially encased composite columns." Journal of Structural Engineering, Vol. 142, Issue, 2, pp. 04015142.1-04015142.9

[16] Pereira, F.M., De Nardin, S., El Debs, L.H.C., (2016). "Structural behaviour of partially encased composite columns under axial loads", Steel and Composite Structures, An International Journal, Vol. 20, Issue. 6, pp. 1305-1322.

[17] Song, Y.C., Wang, R.P., Li, J, (2016). "Local and post-local buckling behavior of welded steel shapes in partially encased composite columns." Thin-Walled Structures, Vol. 108, pp. 93–108.

[18] CSA. (2014), CSA S16–14, "Limit States Design of Steel Structures." Canadian Standards Association, Mississauga, Ontario.

[19] ACI Committee 318. (2008). "Building Code Requirements for Structural Concrete (ACI 318-08) and Commentary (ACI 318R-08)." Farmington Hills, MI: ACI.

[20] ACI. (1997). ACI 363R-92, "State-of-the-art report on high-strength concrete (reapproved in 1997)." American Concrete Institute, Farmington Hills, MI.

[21] ASTM. (2003). A370-03, "Standard test methods and definitions for mechanical testing of steel products." American Society for Testing and Materials, Philadelphia, PA.

[22] Eurocode 4. "Design of composite steel and concrete structures, Part 1-1: General rules and rules for buildings."

[23] Han, L.H., (2002). "Tests on stub columns of concrete-filled RHS sections." Journal of Constructional Steel Research, Vol. 58, Issue. 3, pp. 353–372.